HHS Public Access

Author manuscript

Mol Psychiatry. Author manuscript; available in PMC 2018 May 14.

Published in final edited form as:

Mol Psychiatry. 2018 August ; 23(8): 1798–1806. doi:10.1038/mp.2017.221.

Treating a novel plasticity defect rescues episodic memory in Fragile X model mice

Weisheng Wang, PhD[1,†], **Brittney M. Cox, PhD**[1,†], **Yousheng Jia, PhD**[1], **Aliza A. Le, BS**[1], **Conor D. Cox, BS**[1], **Kwang M. Jung, PhD**[1], **Bowen Hou, BS**[1], **Daniele Piomelli, PhD**[1,2,3], **Christine M. Gall, PhD**[1,4,*], and **Gary Lynch, PhD**[1,5,*]

[1]Department of Anatomy and Neurobiology, University of California, Irvine California 92697

[2]Department of Pharmacology, University of California, Irvine California 92697

[3]Department of Biological Chemistry, University of California, Irvine California 92697

[4]Department of Neurobiology and Behavior, University of California, Irvine California 92697

[5]Department of Psychiatry and Human Behavior, University of California, Irvine California 92697

Abstract

Episodic memory, a fundamental component of human cognition, is significantly impaired in autism. We report the first evidence for this problem in the *Fmr1*-knockout (KO) mouse model of Fragile X syndrome and describe potentially treatable underlying causes. The hippocampus is critical for the formation and use of episodes, with semantic (cue identity) information relayed to the structure via the lateral perforant path (LPP). The unusual form of synaptic plasticity expressed by the LPP (*lpp*LTP) was profoundly impaired in *Fmr1*-KOs relative to wild type mice. Two factors contributed to this defect: i) reduced GluN1 subunit levels in synaptic NMDA receptors and related currents, and ii) impaired retrograde synaptic signaling by the endocannabinoid 2-archadonolglycerol (2-AG). Studies using a novel serial cue paradigm showed that episodic encoding is dependent on both the LPP and the endocannabinoid receptor CB_1, and is strikingly impaired in *Fmr1*-KOs. Enhancing 2-AG signaling rescued both *lpp*LTP and learning in the mutants. Thus, two consequences of the Fragile-X mutation converge on plasticity at one site in hippocampus to prevent encoding of a basic element of cognitive memory. Collectively, the results suggest a clinically plausible approach to treatment.

Introduction

Episodic memory involves the encoding of events into narrative sequences about what happened, where particular features occurred, and the order in which they appeared.[1,2]

[*]Corresponding Authors: C.M. Gall and G. Lynch, To whom correspondence should be addressed: Christine M. Gall, Communicating corresponding author, Department of Anatomy and Neurobiology, University of California at Irvine, 837 Health Sci. Road. Irvine, CA 92697-1275, cmgall@uci.edu, FAX: 949-824-0276.

[†]Indicate equal contributions

Conflict of interest: The authors declare no competing financial interests.

Individuals with intellectual disability, including autism spectrum disorders (ASDs), show specific deficits in the acquisition, recall and integration of episodes, while semantic memory outside of episodes is less affected.[3–12] Aberrant processing of episodes may lead to other cognitive symptomatology associated with autism and related neuropsychiatric conditions.[13]

Despite progress in identifying neurobiological issues associated with various types of learning disorders, little is known about factors related to specific deficits in episodic memory. However, a growing body of evidence indicates that the hippocampus plays a central role in the processing of episodes and thus is a likely site to search for causes.[14–16] Recent work in rodents and humans indicates that the structure receives semantic information ('cue identity') via the lateral entorhinal cortex (LEC) and its lateral perforant path (LPP) projection to the first stage of hippocampal processing, the dentate gyrus.[17] Intriguingly, learning-related synaptic plasticity (long-term potentiation: LTP) in the LPP differs markedly from that expressed by the second cortical input (medial perforant path, MPP) to the dentate gyrus or by connections between hippocampal pyramidal cells. Specifically, LPP potentiation (*lpp*LTP) is initiated postsynaptically through the actions of NMDA and mGluR5 glutamate receptors but expressed presynaptically by an increase in evoked neurotransmitter release[18] with the requisite retrograde messenger being the endocannabinoid 2-arachidonoylglycerol (2-AG).[19,20] This *lpp*LTP is independent of effects on GABAergic neurons, being unaffected by GABA receptor antagonists[23–25]. Plasticity in the LPP is also unusual as it depends on endogenous opioids. The pathway expresses enkephalin[19] and, unlike the MPP, induction of LTP is opioid receptor dependent,[21,22] with the underlying mechanism involving suppression of GABAergic inhibition.[21] The presence of a highly specialized form of plasticity localized to the LPP, 'cue identity' input to hippocampus raises the question of whether defects in this complex synaptic mechanism occur in autism and are associated with a failure to acquire a fundamental element of episodic memory.

The present studies addressed the above possibility using *Fmr1*-KO mice,[23–25] which through a single gene mutation, model the most prevalent monogenetic form of inherited intellectual disability with relatively high comorbidity for ASD.[26,27] We report the first evidence for a pronounced and selective impairment in the acquisition of information in an episodic context in these mutants, accompanied by an equally severe loss of *lpp*LTP. The magnitude of these functional deficits was then traced to disruptions of two distinct components of synaptic signaling. These synaptic disturbances are not specific to the LPP but it is only at this point in hippocampal circuitry that they interact to block learning-related synaptic modifications.

Materials and Methods

Methods are described briefly below, see Supplemental Information for detailed descriptions.

Animals

Studies used male Fmr1-KO mice (sighted FVB 129 background) at 5–8 (field recordings), 4–8 (whole cell recordings) and 8–16 weeks old, and age and background-matched WTs housed 3–5 mice per cage with food and water ad libitum. Experiments were conducted in accordance with NIH guidelines for the Care and Use of Laboratory animals and protocols approved by our Institutional Animal Care and Use Committee.

Electrophysiology

Preparation of hippocampal slices for extracellular field recordings was as described.[18,28] For perforant path components, evoked responses were tested with paired-pulse stimuli to confirm specificity of electrode placement: The LPP and MPP exhibit paired-pulse facilitation and depression, respectively.[18,29] Potentiation was induced using one 100Hz train lasting 1s[21,29] with stimulus duration and intensity increased by 100% and 50% of baseline levels, respectively, and with 10μM picrotoxin (PTX) in the bath.

Whole-cell EPSCs were recorded by clamping granule cells at −70mV in the presence of 50μM PTX to block the contaminating effects of IPSCs. LPP and MPP potentiation was induced using a pairing protocol: 2Hz stimulation for 75s at −10mV holding potential. For the commissural/associational system, optogenetic stimulation was used; potentiation was induced with 2Hz stimulation for 15s at −10mV holding potential.

Drugs

For field recordings: 2-amino-5-phosphonovalerate (APV; 100μM), WIN55,121-2 (5μM), AM251 (5μM), physostigmine (2, 10μM), Clozapine-N-oxide (CNO, 10μM), JZL184 (1μM,), and PTX (10μM). For behavioral studies: AM251 (3 mg/kg), JZL184 (8 mg/kg) and CNO (1,5 mg/kg).

Fluorescence Deconvolution Tomography

Hippocampal slices were processed for immunofluorescence[30] using antisera to GluN1,[31] GluN2A[32] or GluN2B,[33] in combination with anti-PSD-95.[34]

Image z-stacks collected from the dentate gyrus molecular layer were deconvolved and automated systems were used to normalize background density and measure the size and fluorescence intensity of immunolabeled objects.[30,35] Adjacent z-stack montages were digitally stitched together to create a larger dentate molecular layer image from which synaptic elements were quantified for defined lamina.

Lipid Quantitation

Levels of 2-AG, oleoylethanolamide (OEA), arachidonic acid, and stearic acid were determined using liquid chromatography/mass spectrometry (LC/MS) methods.[36,37]

Viral Constructs

Designer Receptors Exclusively Activated by Designed Drug (DREADD) constructs AAV8-CaMKIIa::HA-hM4Di-IRES-mCitrine or AAV-CaMKIIa-HA-hM3D(Gq)-IRES-mCitrine

were injected unilaterally or bilaterally into LEC and/or dentate gyrus. The ChR2 construct, AAV5-CaMKII-hChR2 (H134R)-eYFP-WPRE, was injected bilaterally into CA3.

Odor Discrimination Behavior

Small molecule odorants (see Supplemental Information) were pipetted onto filter paper inside a glass cup with perforated lid. During habituation the mouse was exposed to two cups (without odor) in a Plexiglas box (30x25x21.5 cm) for 5 min. After intervening periods in an identical holding chamber, the mouse was exposed to the two cups containing odors A, B, and C (3 min each). Finally, the mouse was exposed to familiar odor A and novel odor D. Odor exploration was scored when the mouse's nose was within 2cm and directed towards the odor hole. A discrimination index was calculated: (t-novel odor)–(t-familiar odor)/(t-both odors) x100, with 't' denoting the time exploring.

Design elements and statistics

For electrophysiological studies, 'n' was numbers of slices/group from ≥4 mice/group, and groups compared were run in parallel on separate chambers with no specific randomization strategy; effect size was determined on an individual slice basis by comparison of responses during baseline and post-treatment periods. No individual slice results were dropped. For behavioral studies, the goal was n=10–12 mice/group, from at least 2 cohorts, based on past experience; mice were randomly assigned to groups and behavioral assessments were made from videos by investigators blind to treatment. Animals were excluded if object exploration during testing was <1s. For biochemical measures, sample size was based on past experience[18] (no samples excluded). Results are presented as mean ± s.e.m. values and statistics used 2-tail t test unless otherwise specified. The variance within a group and suitability of statistical test was evaluated in all cases. Group sizes are given in the figure captions.

Results

Impaired lppLTP in Fmr1-KOs

Lateral perforant path LTP was tested in acute hippocampal slices from *Fmr1*-KO and wild type (WT) mice. The fEPSP input/output curves were comparable between genotypes (Figure 1a). High frequency, 100Hz stimulation (HFS) elicited robust fEPSP potentiation in WT mice (52.1 ± 3.1% at 55–60 min post-HFS) but much smaller and decremental potentiation in KOs (16.9 ± 2.3%; Figure 1b). Similarly, *lpp*LTP was significantly smaller in whole cell recordings from KOs versus WTs (Figure 1c).

Medial perforant path input/output curves were comparable between genotypes (Figure 1d) as were fEPSP waveforms. MPP potentiation was impaired in *Fmr1*-KOs relative to WTs (Figure 1e), but to a lesser extent than in the LPP (−30.9 ± 11.2% vs. −66.8 ± 6.1%; p=0.01). In whole cell recordings, MPP potentiation was smaller in KOs than WTs but the difference was not significant (Figure 1f). The LTP defect in *Fmr1*-KO MPP observed here is comparable to two previous reports[38,39] but smaller than that in a third.[40]

LTP has not previously been analyzed in the third major input (commissural/associational: C/A) to the granule cells. Channel rhodopsin2 (ChR2) expression and optical stimulation[41,42] were used (Figure 1g) because the diffuse origin and narrow breadth of this projection renders discrete electrical stimulation difficult. Single light flashes produced AMPAR-mediated EPSCs of typical size and shape, with membrane potential at −70mV, and paired-pulse depression (Figure 1h). A train of 30 flashes (2s; membrane potential at −10mV) caused a large increase in EPSCs but the effect decayed steadily over 30 min to baseline. Importantly, C/A potentiation did not differ between WTs and KOs (Figure 1i).

In all, the singular form of LTP expressed in the LPP is impaired in a mouse model of autism to a degree not found in the other excitatory afferents of the dentate gyrus.

NMDAR disturbances in Fmr1-KOs

As *lpp*LTP is completely blocked by NMDA receptor (NMDAR) antagonists,[18,21,43] we tested if loss of the effect in *Fmr1*-KOs is associated with a reduction of NMDAR-gated synaptic currents. EPSCs were recorded in granule cells held at −10mV and −70mV to identify NMDAR and AMPAR currents, respectively[44] (Figure 2a). The AMPAR/NMDAR evoked current ratio was markedly reduced in *Fmr1*-KOs relative to WTs (−58.0 ± 6.3%; Figure 2b).

The NMDAR-mediated component of synaptic responses is also reduced in the MPP,[38] raising the possibility that NMDAR hypo-function is a general feature of *Fmr1*-KO granule cells. However, the AMPAR/NMDAR current ratio was normal for the C/A projection (Figure 2c). Thus, strongly attenuated NMDAR currents in the KOs were restricted to the two branches of the perforant path.

NMDAR subunit levels are reduced in dentate gyrus lysates from *Fmr1*-KO mice,[40] but concentrations of the proteins at perforant path synapses are not known. We used Fluorescence Deconvolution Tomography (FDT) to measure the density of synaptic (i.e., PSD-95 co-localized) NMDAR subunits in the dentate molecular layer (Figure 2d). There was no effect of genotype on numbers of PSD-95-immunopositive clusters in the molecular layer (Figure 2e) or the density frequency distribution for PSD-95 immunolabeling in the outer molecular layer (Figure 2f). However, the density distribution for GluN1 co-localized with PSD-95 was left-shifted in KOs relative to WTs (Figure 2g), indicating lower GluN1 levels at LPP synapses in the mutants. The GluN2A subunit distribution was also left-shifted in KOs but this effect was not significant (Figure 2h) and there were no differences for GluN2B (Figure 2i). Synaptic GluN1 density was also reduced in the middle molecular layer of *Fmr1*-KO mice but, unlike the outer molecular layer, this was also case for GluN2A; GluN2B levels were again not affected by the mutation (Supplementary Figure 1). In all, the Fragile X mutation decreases the concentration of NMDAR subunits, perhaps more severely in MPP than LPP terminal fields.

Learning serial cues is LPP-dependent and impaired in Fmr1-KOs

The LEC is critical for encoding of semantic (‘what’) information contained in episodic memories,[17,45,46] and receives input from association areas of cortex, including a direct projection from piriform (olfactory) cortex. Episodic memory in humans typically is

acquired in the absence of explicit instruction or rewards (unsupervised learning) and is immediately available following exposure to a series of cues. We accordingly developed an olfactory task that incorporates these features to test if *Fmr1*-KOs are impaired in the acquisition of a key element of an episode.

For the Serial odor task, mice were presented with a series of same-odor pairs (i.e., A-A, B-B, C-C) followed by a test trial in which a previously experienced cue was paired with a novel odor ('D'). We also tested simple odor discrimination ('2-cue test')(Figure 3a). In both protocols, WT mice explored the novel odor more than a familiar odor. We then used a chemogenetic, DREADD strategy[47,48] to test if rapid acquisition by WTs in the serial task requires the LPP. An AAV construct supporting expression of an Gi-coupled (inhibitory) DREADD was injected into LEC; expression was evident three weeks later in superficial LEC and the LPP terminal field (Figure 3b) and, as evaluated in hippocampal slices, infusion of the DREADD-specific agonist CNO caused a rapid drop in the size of LPP fEPSPs as anticipated from work on other neuronal systems[49–52] (Figure 3c). Groups of WT mice were prepared with Gi-DREADD transfection of 1) LEC bilaterally or 2) unilateral LEC and contralateral dentate gyrus (i.e., a 'contralateral disconnect' arrangement[53–55] designed to silence LPP activation of the dentate gyrus bilaterally while leaving LEC projections to sites outside the dentate gyrus functional on one side (Figure 3d). Finally, due to occasional missed-injection placements, we obtained data for mice with unilateral Gi-DREADD injection into either LEC or dentate gyrus (Supplementary Figure 3).

Mice were injected with CNO or vehicle 30 min prior to testing. Behavioral results were comparable for mice receiving bilateral LEC and contralateral disconnect DREADD injection placements ($p>0.25$) and, as such, results for these two groups were pooled. In the serial odor task, vehicle-treated mice had a robust discrimination index (DI), denoting learning, whereas serial odor learning was blocked in mice receiving CNO (Figure 3e, left). In contrast, DIs for CNO- and vehicle-treated mice with bilateral Gi-DREADD expression were not different in the '2 cue test' (Figure 3e, right), nor were the total times sampling odors in either the serial (1.6% group difference) or 2-cue (0.5%) paradigm. CNO treatment of mice with unilateral Gi-DREADD transfection of either LEC or dentate gyrus failed to block serial odor learning and CNO did not influence learning in mice without AAV-DREADD infusions (Supplementary Figure 3a,d). In all, these results indicate that serial odor learning in WT mice is dependent upon bilateral function of the LPP projection to the dentate gyrus. There remains a possible contribution from the temporoammonic, LEC to CA3 projection[56] to observed behavioral effects, as these axons arise from the same superficial LEC fields as dentate gyrus afferents, and the Gi-DREADD construct was clearly expressed in projections to both the dentate and distal CA3 fields (Supplemental Figure 3). However, the CA3 pathway would not be affected on one side in the contralateral disconnection mice and we found that unilateral LEC Gi-DREADD injections did not block learning.

Next, we tested if the loss of *lpp*LTP in *Fmr1*-KO mice is accompanied by a comparably severe impairment in LPP-dependent learning. The mutants failed to discriminate between the novel and familiar odors in the serial paradigm (Figure 3f, left), but performed the 2-cue discrimination similarly to WTs ($p=0.84$, Figure 3f, right). *Fmr1*-KOs also spent more time

sampling odor-baited than blank containers and to the same degree as did WTs (Figures 3g,h). These results constitute the first evidence that *Fmr1*-KO mice lack a fundamental requirement for the formation of episodic memory -- encoding the identity of cues within a series.

Defective endocannabinoid signaling contributes to the loss of lppLTP in Fmr1-KO mice

Previous work showed that enhancing cholinergic transmission with physostigmine elevates concentrations of the endocannabinoid 2-AG in hippocampal slices[18] and, via the presynaptic (CB_1R) receptor, depresses release from both medial and lateral perforant paths.[57] We found that the latter CB_1R-dependent effect was substantially reduced in *Fmr1*-KOs relative to WTs in both LPP (Figure 4a,b) and MPP (Figure 4c,d). Next we tested if the physostigmine-induced increase in 2-AG production could offset the *lpp*LTP impairment in *Fmr1*-KO mice. We identified a threshold physostigmine dose that does not reduce LPP synaptic responses (2μM), but nonetheless measurably increases 2-AG levels in WT slices (Supplementary Figures 2a,b,c). Comparable experiments in *Fmr1*-KOs produced two interesting results: 1) baseline levels of 2-AG were significantly lower in KO than WT slices, and 2) physostigmine increased 2-AG in KOs to levels found in untreated WTs**,** although not to the absolute values achieved in treated WTs (Figure 4e). Having identified conditions that normalize 2-AG in *Fmr1*-KO hippocampal slices, we tested for effects on *lpp*LTP and found that 2μM physostigmine more than doubled amplitude of LPP potentiation (Fig 4f).

2-AG is largely degraded in brain by the enzyme monoacylglycerol lipase (MGL), which is localized to axon terminals proximal to CB_1Rs.[58] Treatment with the selective MGL inhibitor JZL184 increases 2-AG levels in the dentate gyrus and enhances *lpp*LTP in WTs.[18] Infusions of JZL184 into *Fmr1*-KO slices restored *lpp*LTP to WT values (Figure 4g), but did not affect potentiation in the MPP (Figure 4h). These results suggest that the presynaptic machinery for expressing *lpp*LTP is not impaired in *Fmr1*-KOs; if so then direct CB_1R stimulation should enhance *lpp*LTP. In accord with this prediction, infusion of CB_1R agonist WIN55,212-2 increased *lpp*LTP in *Fmr1*-KOs (Figure 4i). Conversely, blocking the receptor with the inverse agonist AM251 eliminated the residual LTP in the mutants (Figure 4j).

While the various positive manipulations of endocannabinoid signaling tested here rescued *lpp*LTP in *Fmr1*-KOs (Figure 4k), they did not produce the supra-normal potentiation previously described with such treatments in WTs.[18] We propose that the reduction in postsynaptic NMDAR currents in the KOs places upper limits on the expression of *lpp*LTP.

Normalizing lppLTP rescues serial cue learning in Fmr1-KO mice

We confirmed[18] that *lpp*LTP in WTs is blocked by AM251 (Figure 5a) and then tested for the predicted correspondence between the level of *lpp*LTP and serial cue learning. Peripheral administration of the CB_1R antagonist profoundly reduced retention scores in WTs (Figure 5b). Conversely, treatment with MGL inhibitor JZL184, which enhances 2-AG signaling and *lpp*LTP,[19] restored such learning in *Fmr1*-KOs (Figure 5c). We extended the comparison between the rescue of *lpp*LTP and memory encoding using an LPP-specific manipulation. Past studies demonstrated that DREADD-mediated increases in Gq signaling[59,60] promote LTP in hippocampal field CA1.[51] Thus, Gq-coupled DREADD constructs were injected into

the LEC (Figure 5d) of *Fmr1*-KOs and tests were made for effects of Gq signaling on *lpp*LTP and learning. *Fmr1*-KOs treated with 1 mg/kg CNO before training had substantially higher serial odor retention scores than those receiving vehicle (Figure 5e) with no difference in time sampling the odors (Figure 5f). CNO did not rescue learning in *Fmr1*-KOs with unilateral transfections of the LEC (% time novel vs. familiar, p=0.86, paired t-test, n=7). CNO treatment increased both the amplitude of LPP fEPSPs and the magnitude of *lpp*LTP in hippocampal slices prepared from LEC Gq-DREADD mice (Figure 5g,h). The increase in baseline response produced by the Gq-DREADD agonist was accompanied by a reduction of LPP paired pulse facilitation (Figure 5i), confirming the predicted increase in evoked transmitter release. These results establish that selectively restoring *lpp*LTP with a pathway-specific manipulation suffices to normalize acquisition of 'what' information in *Fmr1*-KO mice.

Discussion

The present findings raise a question of translational importance: to what extent can manipulations targeted at one synaptic defect in a complex system restore normalcy despite the continuing presence of other problems? The results establish that the singular form of plasticity expressed by the pathway conveying the cue identity (semantic) element of episodic memory is inoperative in the *Fmr1*-KO model of intellectual disability associated with ASD. As this element is fundamental to other features (spatial location, temporal order) of an episode, these findings help explain why autistic individuals have difficulty shaping the constant flow of experience into autobiographical narratives.[61–63] A novel, LPP-dependent behavioral task confirmed that *Fmr1*-KO mice are unable to encode the identity of cues embedded in a sequence, while having no difficulty acquiring the same cues when presented outside of a series. Given the magnitude of the impairment, and the short delay between sampling and testing, these results describe one of the most severe learning deficits so far reported for *Fmr1*-KOs. Whether the defects involve primacy vs. recency of the cues, a distinction reported for hippocampal damage[64] and autism[65], is an important question for future research.

The Fragile X mutation disturbs a large number of neurobiological processes throughout the brain[66–68] and yet its effects on behavior within an individual can range from subtle to obvious.[69,70] One explanation for this uneven effect is that major problems emerge only at sites where multiple perturbations converge on specialized functions. This appears to be the case for the perforant path innervation of the dentate gyrus. We identified two distinct defects in *Fmr1*-KOs, one relating to NMDARs and the second to endocannabinoid signaling. Both the medial and lateral perforant paths expressed these impairments, but reductions in plasticity were clearly different. Prior work helps explain these surprising results: both inputs depend on NMDARs to generate activity-driven synaptic modifications, [21,40] but potentiation in the LPP alone requires endocannabinoid signaling.[18] The convergence of defects in these two factors is a singular feature of the LPP, resulting in an unusually severe, Fragile X-related LTP impairment. In accord with this, the decremental form of potentiation described here for the third (C/A) input to the dentate gyrus was not detectably affected by the *Fmr1* mutation.

Deficient NMDAR currents and endocannabinoid signaling in *Fmr1*-KOs did not appear to be secondary to generalized synaptic disturbances: there were no detectable changes to baseline synaptic responses, numbers of excitatory synaptic contacts, or the per-synapse density of PSD-95. The relatively discrete nature of LPP abnormalities in *Fmr1*-KO mice raised the question of whether treatments specifically targeted to just one of them could normalize plasticity. Tests of this critical point showed that enhancing 2-AG signaling restored *lpp*LTP to levels found in untreated WTs. The three effective treatments included manipulations that increase the production of 2-AG, slow its breakdown, or directly stimulate its target receptor. Importantly, these results suggest that the presynaptic machinery that expresses and stabilizes the potentiated state of LPP terminals is largely intact in *Fmr1*-KOs. Whether agents addressing reduced NMDAR functioning also rescue *lpp*LTP despite problems with the 2-AG system remains to be tested. Positive results would open the potential for corrective synergies between two agents administered at sub-threshold concentrations. Relatedly, therapeutics pertinent to the manipulations used in the present study are either being considered (MGL inhibitors)[71] or are in use (physostigmine variants)[72,73] for conditions other than autism.

There remained the question of whether correcting the loss of plasticity in the LPP of *Fmr1*-KOs is by itself sufficient to rescue episodic encoding. We addressed this issue by selectively transfecting the LEC-dentate gyrus system with a Gq-DREADD, a preparation that allowed for discrete and transient facilitation of activity in the LPP without alterations to other brain areas. This manipulation proved sufficient to restore *lpp*LTP and to normalize learning in a serial cue paradigm. Together the results point to the surprising conclusion that a severe problem in a fundamental episodic memory operation, as found in ASD,[13] and described here in a mouse model of the condition, can be traced to defects in an unusual form of plasticity localized to a single site within hippocampus.

In all, this work extends the analysis of a prominent cognitive feature of autism to an animal model, links the observed behavioral abnormality to converging signaling defects in a particular network node, and points to a plausible therapeutic strategy.

Supplementary Material

Refer to Web version on PubMed Central for supplementary material.

Acknowledgments

Funding: This research was funded by National Institutes of Health grants NS045260, NS085709 and HD089491 to C.M.G. and G.L., and DA-012413 and DA031387 to D.P., Department of Defense Multidisciplinary University Research Initiative Grant N00014-101-0072 from the Office of Naval Research to G.L.; UL1 TR001414 fellowship to B.M.C., and National Science Foundation fellowship DGE0808392 to C.D.C.

References

1. Hampton RR, Schwartz BL. Episodic memory in nonhumans: what, and where, is when? Curr Opin Neurobiol. 2004; 14:192–197. [PubMed: 15082324]
2. Tulving E. Eisodic and semantic memory. In: Tulving E, Donaldson W, editorsOrganization of Memory. Academic Press; New York: 1972. 381–403.

3. Grober E, Hall CB, Lipton RB, Zonderman AB, Resnick SM, Kawas C. Memory impairment, executive dysfunction, and intellectual decline in preclinical Alzheimer's disease. J Int Neuropsychol Soc. 2008; 14:266–278. [PubMed: 18282324]
4. Leyhe T, Muller S, Milian M, Eschweiler GW, Saur R. Impairment of episodic and semantic autobiographical memory in patients with mild cognitive impairment and early Alzheimer's disease. Neuropsychologia. 2009; 47:2464–2469. [PubMed: 19409401]
5. Xie SX, Libon DJ, Wang X, Massimo L, Moore P, Vesely L, et al. Longitudinal patterns of semantic and episodic memory in frontotemporal lobar degeneration and Alzheimer's disease. J Int Neuropsychol Soc. 2010; 16:278–286. [PubMed: 20003584]
6. Schneider A, Hagerman RJ, Hessl D. Fragile X syndrome -- from genes to cognition. Dev Disabil Res Rev. 2009; 15:333–342. [PubMed: 20014363]
7. Gaigg SB, Bowler DM, Ecker C, Calvo-Merino B, Murphy DG. Episodic Recollection Difficulties in ASD Result from Atypical Relational Encoding: Behavioral and Neural Evidence. Autism Res. 2015; 8:317–327. [PubMed: 25630307]
8. Crane L, Goddard L. Episodic and semantic autobiographical memory in adults with autism spectrum disorders. J Autism Dev Disord. 2008; 38:498–506. [PubMed: 17668308]
9. Crane L, Lind SE, Bowler DM. Remembering the past and imagining the future in autism spectrum disorder. Memory. 2013; 21:157–166. [PubMed: 22901078]
10. Gaigg SB, Bowler DM, Gardiner JM. Episodic but not semantic order memory difficulties in autism spectrum disorder: evidence from the Historical Figures Task. Memory. 2014; 22:669–678. [PubMed: 23815188]
11. Hare DJ, Mellor C, Azmi S. Episodic memory in adults with autistic spectrum disorders: recall for self- versus other-experienced events. Res Dev Disabil. 2007; 28:317–329. [PubMed: 16839739]
12. Lind SE, Williams DM, Bowler DM, Peel A. Episodic memory and episodic future thinking impairments in high-functioning autism spectrum disorder: an underlying difficulty with scene construction or self-projection? Neuropsychology. 2014; 28:55–67. [PubMed: 24015827]
13. Souchay C, Guillery-Girard B, Pauly-Takacs K, Wojcik DZ, Eustache F. Subjective experience of episodic memory and metacognition: a neurodevelopmental approach. Front Behav Neurosci. 2013; 7:212. [PubMed: 24399944]
14. Burgess N, Maguire EA, O'Keefe J. The human hippocampus and spatial and episodic memory. Neuron. 2002; 35:625–641. [PubMed: 12194864]
15. Dickerson BC, Eichenbaum H. The episodic memory system: neurocircuitry and disorders. Neuropsychopharmacology. 2010; 35:86–104. [PubMed: 19776728]
16. Wixted JT, Squire LR, Jang Y, Papesh MH, Goldinger SD, Kuhn JR, et al. Sparse and distributed coding of episodic memory in neurons of the human hippocampus. Proc Natl Acad Sci U S A. 2014; 111:9621–9626. [PubMed: 24979802]
17. Reagh ZM, Yassa MA. Object and spatial mnemonic interference differentially engage lateral and medial entorhinal cortex in humans. Proc Natl Acad Sci U S A. 2014; 111:E4264–4273. [PubMed: 25246569]
18. Wang W, Trieu BH, Palmer LC, Jia Y, Pham DT, Jung KM, et al. A primary cortical input to hippocampus expresses a pathway-specific and endocannabinoid-dependent form of long-term potentiation. eNeuro. 2016:3.
19. Devane WA, Hanus L, Breuer A, Pertwee RG, Stevenson LA, Griffin G, et al. Isolation and structure of a brain constituent that binds to the cannabinoid receptor. Science. 1992; 258:1946–1949. [PubMed: 1470919]
20. Stella N, Schweitzer P, Piomelli D. A second endogenous cannabinoid that modulates long-term potentiation. Nature. 1997; 388:773–778. [PubMed: 9285589]
21. Bramham CR, Sarvey JM. Endogenous activation of mu and delta-1 opioid receptors is required for long-term potentiation induction in the lateral perforant path: dependence on GABAergic inhibition. J Neurosci. 1996; 16:8123–8131. [PubMed: 8987837]
22. Breindl A, Derrick BE, Rodriguez SB, Martinez JL Jr. Opioid receptor-dependent long-term potentiation at the lateral perforant path-CA3 synapse in rat hippocampus. Brain Res Bull. 1994; 33:17–24. [PubMed: 8275323]

23. Dolen G, Bear MF. Role for metabotropic glutamate receptor 5 (mGluR5) in the pathogenesis of fragile X syndrome. J Physiol. 2008; 586:1503–1508. [PubMed: 18202092]
24. Bhakar AL, Dolen G, Bear MF. The pathophysiology of fragile X (and what it teaches us about synapses). Annu Rev Neurosci. 2012; 35:417–443. [PubMed: 22483044]
25. Santoro MR, Bray SM, Warren ST. Molecular mechanisms of fragile X syndrome: a twenty-year perspective. Annu Rev Pathol. 2012; 7:219–245. [PubMed: 22017584]
26. Wadell PM, Hagerman RJ, Hessl DR. Fragile X Syndrome: Psychiatric Manifestations, Assessment and Emerging Therapies. Curr Psychiatry Rev. 2013; 9:53–58. [PubMed: 25632275]
27. Yu TW, Berry-Kravis E. Autism and fragile X syndrome. Semin Neurol. 2014; 34:258–265. [PubMed: 25192504]
28. Trieu BH, Kramar EA, Cox CD, Jia Y, Wang W, Gall CM, et al. Pronounced differences in signal processing and synaptic plasticity between piriform-hippocampal network stages: a prominent role for adenosine. J Physiol. 2015; 593:2889–2907. [PubMed: 25902928]
29. Christie BR, Abraham WC. Differential regulation of paired-pulse plasticity following LTP in the dentate gyrus. Neuroreport. 1994; 5:385–388. [PubMed: 8003660]
30. Seese RR, Babayan AH, Katz AM, Cox CD, Lauterborn JC, Lynch G, et al. LTP induction translocates cortactin at distant synapses in wild-type but not Fmr1 knock-out mice. J Neurosci. 2012; 32:7403–7413. [PubMed: 22623686]
31. Kahlfuss S, Simma N, Mankiewicz J, Bose T, Lowinus T, Klein-Hessling S, et al. Immunosuppression by N-methyl-D-aspartate receptor antagonists is mediated through inhibition of Kv1.3 and KCa3. 1 channels in T cells. Mol Cell Biol. 2014; 34:820–831. [PubMed: 24344200]
32. Larsen RS, Corlew RJ, Henson MA, Roberts AC, Mishina M, Watanabe M, et al. NR3A-containing NMDARs promote neurotransmitter release and spike timing-dependent plasticity. Nat Neurosci. 2011; 14:338–344. [PubMed: 21297630]
33. Zhang J, Diamond JS. Subunit- and pathway-specific localization of NMDA receptors and scaffolding proteins at ganglion cell synapses in rat retina. J Neurosci. 2009; 29:4274–4286. [PubMed: 19339621]
34. Takahashi H, Arstikaitis P, Prasad T, Bartlett TE, Wang YT, Murphy TH, et al. Postsynaptic TrkC and presynaptic PTPsigma function as a bidirectional excitatory synaptic organizing complex. Neuron. 2011; 69:287–303. [PubMed: 21262467]
35. Seese RR, Chen LY, Cox CD, Schulz D, Babayan AH, Bunney WE, et al. Synaptic abnormalities in the infralimbic cortex of a model of congenital depression. J Neurosci. 2013; 33:13441–13448. [PubMed: 23946402]
36. Jung KM, Clapper JR, Fu J, D'Agostino G, Guijarro A, Thongkham D, et al. 2-arachidonoylglycerol signaling in forebrain regulates systemic energy metabolism. Cell Metab. 2012; 15:299–310. [PubMed: 22405068]
37. Jung KM, Astarita G, Zhu C, Wallace M, Mackie K, Piomelli D. A key role for diacylglycerol lipase-alpha in metabotropic glutamate receptor-dependent endocannabinoid mobilization. Mol Pharmacol. 2007; 72:612–621. [PubMed: 17584991]
38. Eadie BD, Cushman J, Kannangara TS, Fanselow MS, Christie BR. NMDA receptor hypofunction in the dentate gyrus and impaired context discrimination in adult Fmr1 knockout mice. Hippocampus. 2012; 22:241–254. [PubMed: 21049485]
39. Yun SH, Trommer BL. Fragile X mice: reduced long-term potentiation and N-Methyl-D-Aspartate receptor-mediated neurotransmission in dentate gyrus. J Neurosci Res. 2011; 89:176–182. [PubMed: 21162125]
40. Bostrom CA, Majaess NM, Morch K, White E, Eadie BD, Christie BR. Rescue of NMDAR-dependent synaptic plasticity in Fmr1 knock-out mice. Cereb Cortex. 2015; 25:271–279. [PubMed: 23968838]
41. Zhang F, Wang LP, Boyden ES, Deisseroth K. Channelrhodopsin-2 and optical control of excitable cells. Nat Methods. 2006; 3:785–792. [PubMed: 16990810]
42. Roy DS, Arons A, Mitchell TI, Pignatelli M, Ryan TJ, Tonegawa S. Memory retrieval by activating engram cells in mouse models of early Alzheimer's disease. Nature. 2016; 531:508–512. [PubMed: 26982728]

43. Hanse E, Gustafsson B. Long-term Potentiation and Field EPSPs in the Lateral and Medial Perforant Paths in the Dentate Gyrus In Vitro: a Comparison. Eur J Neurosci. 1992; 4:1191–1201. [PubMed: 12106423]
44. Jia Y, Gall CM, Lynch G. Presynaptic BDNF promotes postsynaptic long-term potentiation in the dorsal striatum. J Neurosci. 2010; 30:14440–14445. [PubMed: 20980601]
45. Kim WR, Lee JW, Sun W, Lee SH, Choi JS, Jung MW. Effect of dentate gyrus disruption on remembering what happened where. Front Behav Neurosci. 2015; 9:170. [PubMed: 26175676]
46. Wilson DI, Watanabe S, Milner H, Ainge JA. Lateral entorhinal cortex is necessary for associative but not nonassociative recognition memory. Hippocampus. 2013; 23:1280–1290. [PubMed: 23836525]
47. Dong S, Allen JA, Farrell M, Roth BL. A chemical-genetic approach for precise spatio-temporal control of cellular signaling. Mol Biosyst. 2010; 6:1376–1380. [PubMed: 20532295]
48. Zhu H, Roth BL. Silencing synapses with DREADDs. Neuron. 2014; 82:723–725. [PubMed: 24853931]
49. Zhu H, Pleil KE, Urban DJ, Moy SS, Kash TL, Roth BL. Chemogenetic inactivation of ventral hippocampal glutamatergic neurons disrupts consolidation of contextual fear memory. Neuropsychopharmacology. 2014; 39:1880–1892. [PubMed: 24525710]
50. Robinson S, Todd TP, Pasternak AR, Luikart BW, Skelton PD, Urban DJ, et al. Chemogenetic silencing of neurons in retrosplenial cortex disrupts sensory preconditioning. J Neurosci. 2014; 34:10982–10988. [PubMed: 25122898]
51. Lopez AJ, Kramar E, Matheos DP, White AO, Kwapis J, Vogel-Ciernia A, et al. Promoter-Specific Effects of DREADD Modulation on Hippocampal Synaptic Plasticity and Memory Formation. J Neurosci. 2016; 36:3588–3599. [PubMed: 27013687]
52. Stachniak TJ, Ghosh A, Sternson SM. Chemogenetic synaptic silencing of neural circuits localizes a hypothalamus-->midbrain pathway for feeding behavior. Neuron. 2014; 82:797–808. [PubMed: 24768300]
53. Mahler SV, Vazey EM, Beckley JT, Keistler CR, McGlinchey EM, Kaufling J, et al. Designer receptors show role for ventral pallidum input to ventral tegmental area in cocaine seeking. Nat Neurosci. 2014; 17:577–585. [PubMed: 24584054]
54. Eldridge MA, Lerchner W, Saunders RC, Kaneko H, Krausz KW, Gonzalez FJ, et al. Chemogenetic disconnection of monkey orbitofrontal and rhinal cortex reversibly disrupts reward value. Nat Neurosci. 2016; 19:37–39. [PubMed: 26656645]
55. Lex B, Hauber W. Disconnection of the entorhinal cortex and dorsomedial striatum impairs the sensitivity to instrumental contingency degradation. Neuropsychopharmacology. 2010; 35:1788–1796. [PubMed: 20357754]
56. Witter MP. Organization of the entorhinal-hippocampal system: a review of current anatomical data. Hippocampus. 1993; 3:33–44. [PubMed: 8287110]
57. Colgin LL, Kramar EA, Gall CM, Lynch G. Septal modulation of excitatory transmission in hippocampus. J Neurophysiol. 2003; 90:2358–2366. [PubMed: 12840078]
58. Gulyas AI, Cravatt BF, Bracey MH, Dinh TP, Piomelli D, Boscia F, et al. Segregation of two endocannabinoid-hydrolyzing enzymes into pre- and postsynaptic compartments in the rat hippocampus, cerebellum and amygdala. Eur J Neurosci. 2004; 20:441–458. [PubMed: 15233753]
59. Zhu H, Roth BL. DREADD: a chemogenetic GPCR signaling platform. Int J Neuropsychopharmacol. 2014:18.
60. Sternson SM, Roth BL. Chemogenetic tools to interrogate brain functions. Annu Rev Neurosci. 2014; 37:387–407. [PubMed: 25002280]
61. Davachi L, DuBrow S. How the hippocampus preserves order: the role of prediction and context. Trends Cogn Sci. 2015; 19:92–99. [PubMed: 25600586]
62. Devito LM, Eichenbaum H. Memory for the order of events in specific sequences: contributions of the hippocampus and medial prefrontal cortex. J Neurosci. 2011; 31:3169–3175. [PubMed: 21368028]
63. Manns JR, Howard MW, Eichenbaum H. Gradual changes in hippocampal activity support remembering the order of events. Neuron. 2007; 56:530–540. [PubMed: 17988635]

64. Hermann BP, Seidenberg M, Wyler A, Davies K, Christeson J, Moran M, et al. The effects of human hippocampal resection on the serial position curve. Cortex. 1996; 32:323–334. [PubMed: 8800618]

65. Bowler DM, Limoges E, Mottron L. Different verbal learning strategies in autism spectrum disorder: evidence from the Rey Auditory Verbal Learning Test. J Autism Dev Disord. 2009; 39:910–915. [PubMed: 19205859]

66. Ghosh A, Michalon A, Lindemann L, Fontoura P, Santarelli L. Drug discovery for autism spectrum disorder: challenges and opportunities. Nat Rev Drug Discov. 2013; 12:777–790. [PubMed: 24080699]

67. Maurin T, Zongaro S, Bardoni B. Fragile X Syndrome: from molecular pathology to therapy. Neurosci Biobehav Rev. 2014; 46(Pt 2):242–255. [PubMed: 24462888]

68. Richter JD, Bassell GJ, Klann E. Dysregulation and restoration of translational homeostasis in fragile X syndrome. Nat Rev Neurosci. 2015; 16:595–605. [PubMed: 26350240]

69. McNaughton CH, Moon J, Strawderman MS, Maclean KN, Evans J, Strupp BJ. Evidence for social anxiety and impaired social cognition in a mouse model of fragile X syndrome. Behav Neurosci. 2008; 122:293–300. [PubMed: 18410169]

70. Santos AR, Kanellopoulos AK, Bagni C. Learning and behavioral deficits associated with the absence of the fragile X mental retardation protein: what a fly and mouse model can teach us. Learn Mem. 2014; 21:543–555. [PubMed: 25227249]

71. Saario SM, Laitinen JT. Therapeutic potential of endocannabinoid-hydrolysing enzyme inhibitors. Basic Clin Pharmacol Toxicol. 2007; 101:287–293. [PubMed: 17910610]

72. Davis KL, Mohs RC. Enhancement of memory processes in Alzheimer's disease with multiple-dose intravenous physostigmine. Am J Psychiatry. 1982; 139:1421–1424. [PubMed: 6753611]

73. Francis PT, Palmer AM, Snape M, Wilcock GK. The cholinergic hypothesis of Alzheimer's disease: a review of progress. J Neurol Neurosurg Psychiatry. 1999; 66:137–147. [PubMed: 10071091]

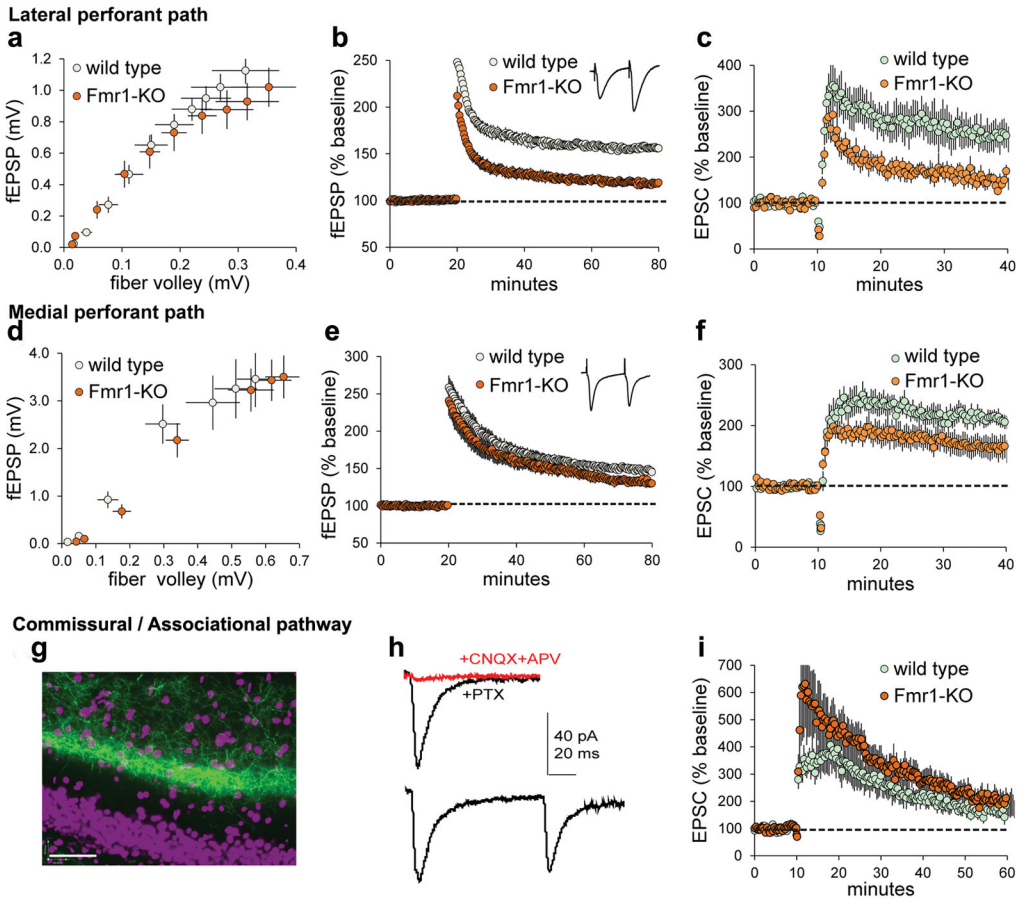

Figure 1. Lateral perforant path LTP is markedly impaired in *Fmr1*-KOs

Acute hippocampal slices were used to evaluate the effect of genotype on LTP of DG afferents using field (a,b,d,e) and whole cell (c,f,h,i) recordings. (**a–c**) The LPP input/output (I/O) curve was comparable between genotypes (a, p=0.99, $F_{(9,220)}$=0.09, n=12 WT, n=10 KO) whereas *Fmr1*-KO LPP potentiation was impaired in fEPSP (b, p<0.0001, $t_{(26)}$=8.96, n=13 WT, n=15 KO) and whole cell (c, p=0.002, n=7 ea) recordings. (**d–f**) For the medial perforant path, the I/O curve showed no effect of genotype (d, p=0.99, $F_{(6,140)}$=0.16, n=11 ea) and LTP was only modestly impaired in WT vs KO fEPSP (e, p=0.029, $t_{(34)}$=2.28, n=20 WT, n=16 KO) and whole cell recordings (f, p>0.05, n=10 ea). (**g–i**) Commissural/ associational (C/A) responses were evaluated using optical stimulation of channelrhodopsin (ChR2) expressing afferents. (**g**) Image shows ChR2-GFP labeling of C/A afferents (cell nuclei purple; bar=40μm); (**h**) light-generated responses recorded from granule cells clamped at −70mV are glutamate receptor-dependent (top: Not blocked by 50μM PTX but eliminated by CNQX+APV) and exhibit paired-pulse depression (bottom). (**i**) Repeated optical stimulation of ChR2-loaded C/A afferents potentiates the postsynaptic (clamped granule cell) response to comparable levels in the two genotypes as assessed during last 5 min of recording (p=0.68, $t_{(14)}$=0.41, n=7 WT, n=9 KO). t-tests (b,e), U-test (c,f), and 2-way ANOVA (a,d).

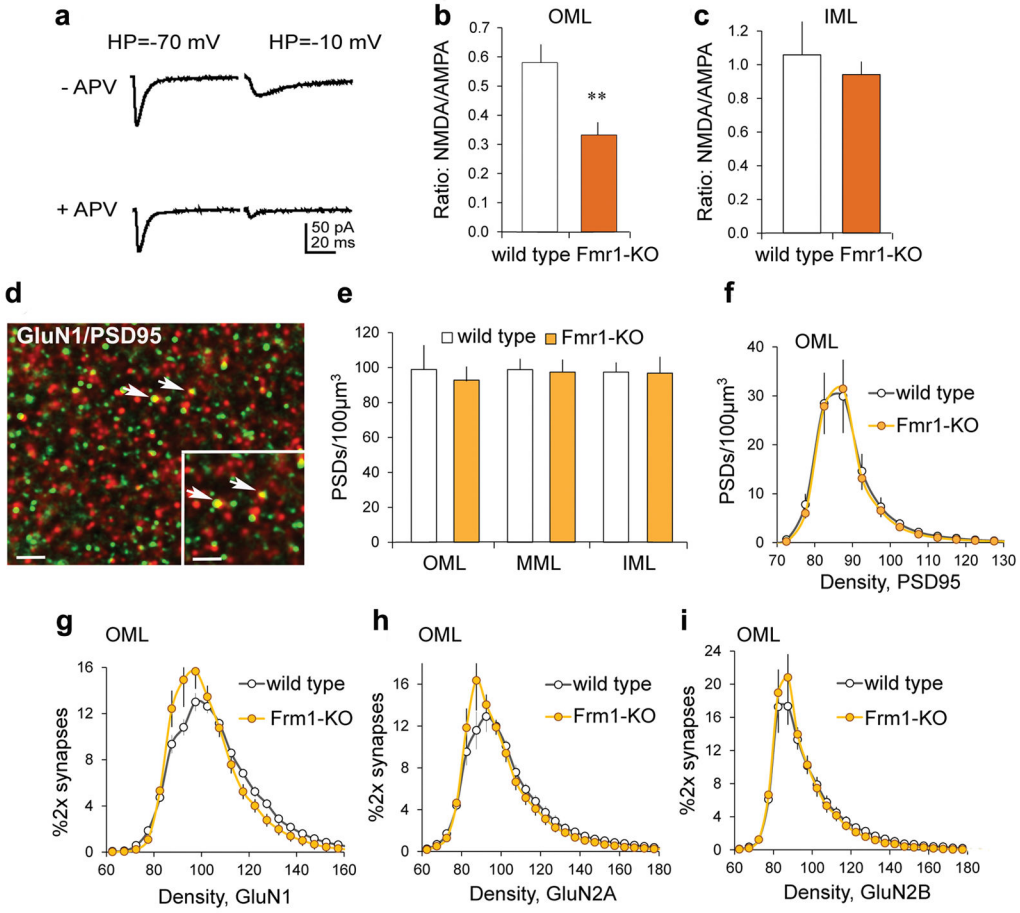

Figure 2. NMDAR currents and GluN1 levels in the LPP field are reduced in *Fmr1*-KO relative to WT mice

(**a**) To assess NMDAR/AMPAR current ratios, EPSCs were measured with the membrane potential at −10mV and −70mV, with and without NMDAR antagonist APV present. **(b,c)** The AMPAR to NMDAR evoked current ratio was lower in *Fmr1*-KOs vs WTs for the outer molecular layer (OML, **p=0.007, $t_{(10)}$=3.17, n=6 ea), but not the inner molecular layer (IML, p=0.58, $t_{(10)}$=0.57, n=6 ea). **(d)** Deconvolved image shows immunofluorescent localization of GluN1 (red) and PSD-95 (green): Yellow and arrows indicate double-labeling (bar=10µm; inset bar=2µm). **(e)** Numbers of PSD-95+ synapses were not different across molecular layer lamina between WTs and KOs (OML: p=0.45, $t_{(14)}$=0.79; middle molecular layer, MML: p=0.77, $t_{(14)}$=0.30; IML: p=0.92, $t_{(14)}$=0.10; n=7 WT, n=9 KO). **(f)** For the same samples, there was no effect of genotype for PSD-95 immunolabeling density frequency distributions in the OML (p=1.00, $F_{(23,322)}$=0.27). **(g–i)** Immunolabeling density frequency distributions for PSD-95 colocalized GluN1 in the OML were left-shifted in KOs vs WTs (g: p<0.0001, $f_{(23,322)}$=3.82, n=7 WT, n=8 KO); curves for GluN2A and GluN2B did not differ between genotypes (h: p=0.18, $F_{(26,416)}$=1.25, n=9 ea; i: p=0.99, $F_{(27,486)}$=0.43, n=9 WT, n=11 KO). t-test (b,c,e); 2-way ANOVA (f–i).

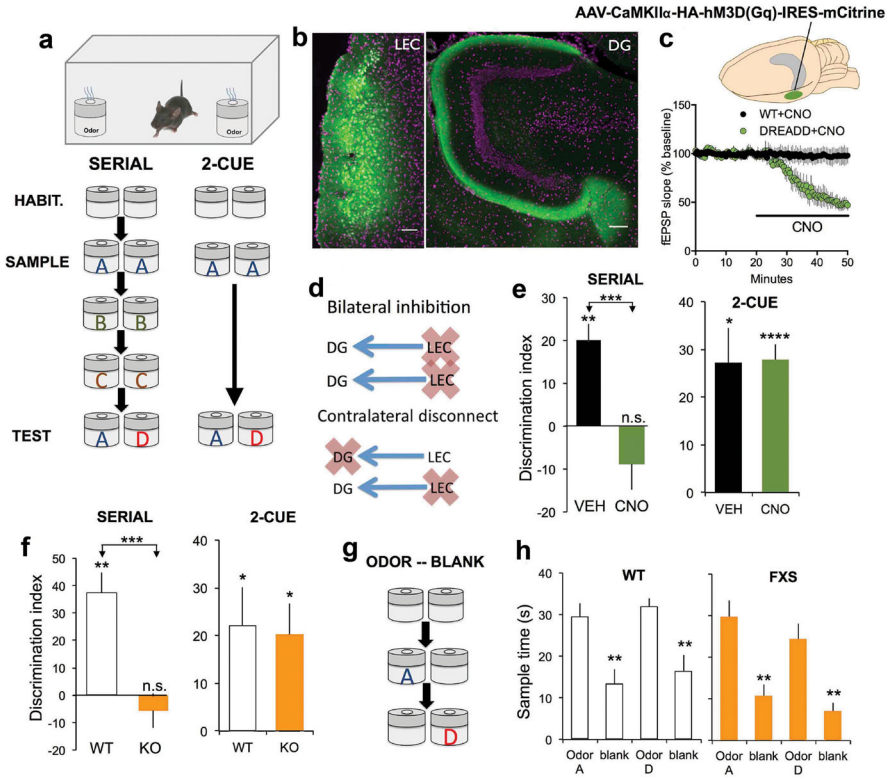

Figure 3. Serial odor learning is dependent on the LPP and impaired in *Fmr1*-KOs

(**a**) Behavioral paradigms. *Serial*: Mice were allowed to habituate (3 min) to the chamber with two identical containers, and then returned to the chamber containing containers scented with identical odor pairs (A:A, B:B, C:C) for 3 min trials spaced by 2 min; for the 'test' trial 5 min later mice were exposed to containers containing familiar odor'A' and novel odor ('D'). *2 Cue*: Mice were exposed to one odor pair ('A:A') then tested for sampling times when familiar 'A' was paired with novel odor 'D'. The delay between "A:A" sampling and 'A' vs. 'D' testing was the same as in the serial protocol. (**b**) An AAV-Gi-DREADD was injected into lateral entorhinal cortex (LEC, left) resulting in dense mCitrine-labeling of LEC neurons and their LPP projections to the dentate gyrus (DG, right; bars=150 μm). (**c**) CNO infused into LPP Gi-DREADD hippocampal slices rapidly suppressed LPP fEPSPs (p=0.0008, n=4 ea). (**d**) Gi-DREADD protocols: bilateral LEC transfection ('bilateral inhibition') or unilateral LEC and contralateral DG transfection ('contralateral disconnect'). (**e**) *Left*: LEC-Gi-DREADD mice were tested in the Serial paradigm after vehicle (VEH) or CNO treatment: VEH-mice spent 61.5 ± 12% more time sampling the novel than the familiar odor (**p<0.002, n=20); this bias was absent in CNO-mice ; 'n.s.', p=0.45, n=18; ***p=0.0002). *Right*. Both groups recognized the novel odor in the 2-cue paradigm (*p=0.014, ****p=0.00003, paired). (**f**) WT mice (n=10) learned (preferred novel odor) the serial task whereas KOs (n=11) did not (***p=0.0004). *Right*. WTs (n=12) and KOs (n=16) both learned the 2-cue test (*p<0.05). (**g**) Protocol for sample odor vs blank container comparison with timing as in the *Serial* task. (**h**) Both WTs (n=8) and *Fmr1*-KOs (n=5) spent more time sampling odors than blank containers (**p<0.01, paired; no effect of genotype, 2-way ANOVA: interaction p=0.50; groups p=0.20). t-tests (c,e,f).

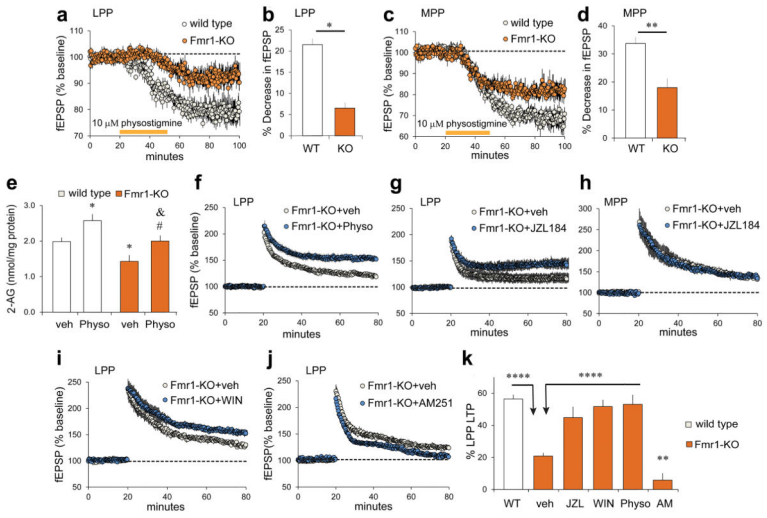

Figure 4. *Fmr1*-KO 2-AG signaling is defective but its activation can rescue *lpp*LTP

(a–d) Physostigmine reduced fEPSPs in WT and, to lesser extent, *Fmr1*-KO LPP (a: p=0.012, $t_{(10)}$=3.03; b: *p=0.02, $t_{(10)}$=2.80; n=6 ea) and MPP (c: p=0.009, $t_{(10)}$=3.26; d: **p=0.003, $t_{(10)}$=3.96; n=6 ea)**. (e)** Physostigmine (Physo; 2μM, 1h) increased 2-AG levels in WTs and KOs but did not eliminate effect of genotype (p=0.0002, $F_{(3,38)}$=8.41; *p<0.05 vs WT+veh; $^{\#}$p<0.05 vs KO+veh; $^{\&}$p<0.05 vs WT+Physo; n=9 KO+veh, n=10 others). **(f–j)** *Fmr1*-KO slices were infused with compounds beginning 0.5 h before baseline recordings; high-frequency stimulation was applied at the 20 min mark. (**f,g**) Physostigmine (f) and JZL184 (g) increased *lpp*LTP magnitude (f, p=0.02, $t_{(19)}$=2.47, n=11 veh, n=10 Physo; g, p=0.008, $t_{(24)}$=2.89, n=11 veh, n=15 JZL). (**h**) JZL184 did not influence MPP potentiation (p=0.25, $t_{(12)}$=1.22, n=7 ea). (**i**) WIN55,212-2 (WIN, 5μM) increased *Fmr1*-KO *lpp*LTP magnitude (p=0.002, $t_{(18)}$=4.56, n=10 ea). (**j**) AM251 (5μM) eliminated the modest *lpp*LTP in *Fmr1*-KOs (p=0.007, $t_{(13)}$=3.23, n=8 veh, n=7 AM251). **(k)** Manipulations that increase 2-AG rescue *Fmr1*-KO *lpp*LTP (p<0.0001, $F_{(5,102)}$=22.19; ****p<0.0001; $^{\#\#}$p<0.01 vs KO +veh). One way ANOVA with Newman-Keuls (e,k) and t-test (b,d).

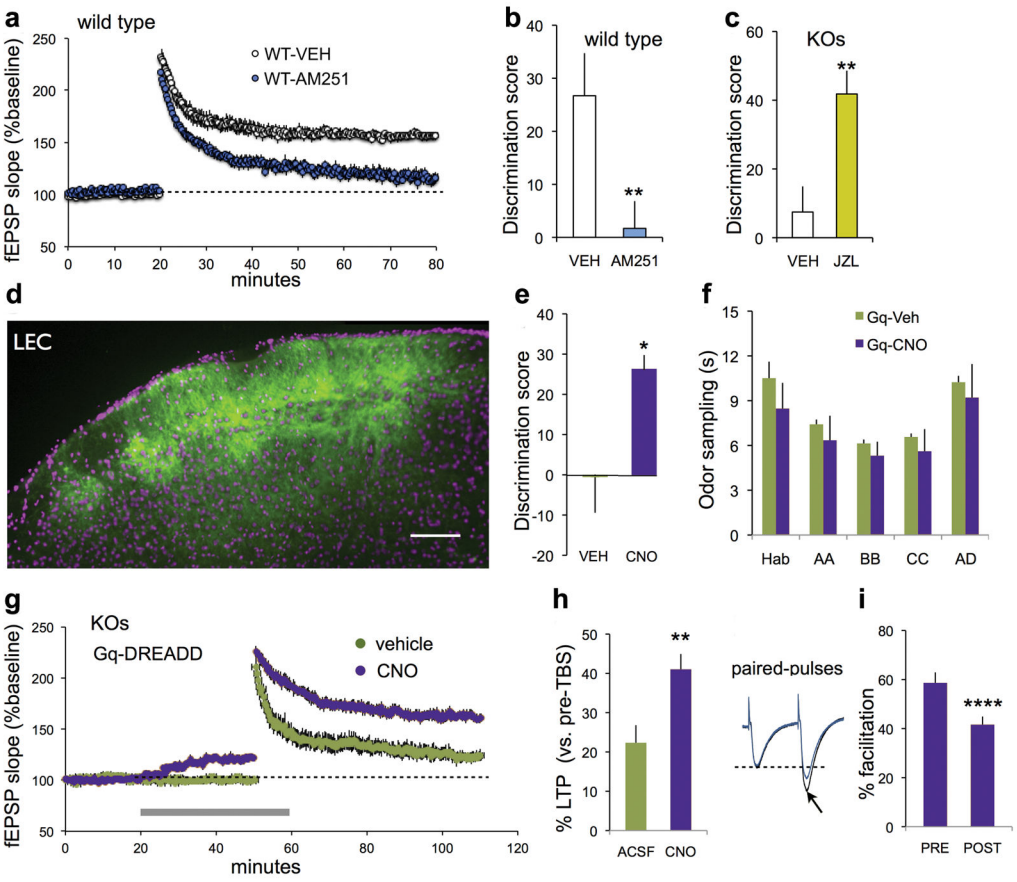

Figure 5. Treatments that normalize *lpp*LTP rescue learning in *Fmr1*-KOs

(**a,b**) In hippocampal slices from wild type (WT) mice, AM251 blocked both *lpp*LTP (a, $p<0.0001$ vs vehicle (VEH), $t_{(16)}=8.44$, n=10 WT-VEH, n=8 WT-AM251) and serial odor acquisition (b, **p=0.018, n=11 WT-VEH, n=8 WT-AM251). (**c**) Treatment with JZL184 (JZL) fully rescued *Fmr1*-KO serial odor learning (*p=0.004 vs VEH, n=9 VEH; n=8 JZL). (**d**) Representative AAV-Gq-DREADD injection in lateral entorhinal cortex (LEC) shows mCitrine expression in superficial layers (bar: 100 μm). (**e,f**) CNO restored serial odor learning in LEC-Gq DREADD *Fmr1*-KOs (e, p=0.046; n=11 VEH, n=6 CNO), without influencing total odor sampling times (f, p=0.419 (treatment), two-way RM ANOVA). (**g**) For *Fmr1*-KOs with LPP Gq-DREADD expression, CNO (gray bar) increased baseline LPP fEPSP slope, and the magnitude and stability *lpp*LTP; vehicle did not influence either measure (n=6 ea). (**h**) Percent *lpp*LTP (last 5 min of recording) was greater for CNO vs vehicle/ACSF-slices (**p=0.01). (**i**) Paired-pulse facilitation in Gq-DREADD expressing LPP was reduced by CNO infusion (*Fmr1*-KO slices; 40 ms interpulse interval; ****p=0.0001). t-tests for b,c,e,h and i.